KSME

Springer

Journal of Mechanical Science and Technology 34 (10) 2020

Original Article
DOI 10.1007/s12206-020-0917-6

Keywords:
· Sheet forming
· CNC incremental forming
· Combinatorial optimization of sheet postures
· Thickness uniformity

Correspondence to:
Hu Zhu
zhuhu10@163.com

Citation:
Zhu, H., Wang, Y., Kang, J. (2020). Research on combinatorial optimization of multidirectional sheet postures for forming thickness uniformity. Journal of Mechanical Science and Technology 34 (10) (2020) 4251~4261.
http://doi.org/10.1007/s12206-020-0917-6

Received May 10th, 2020
Revised July 16th, 2020
Accepted August 4th, 2020

† Recommended by Editor Hyung Wook Park

Research on combinatorial optimization of multidirectional sheet postures for forming thickness uniformity

Hu Zhu[1], Yang Wang[1] and Jaeguan Kang[2]

[1]College of Mechanical and Electrical Engineering, Shenyang Aerospace University, Shenyang, Liaoning 110136, China, [2]School of Mechanical and Automation Engineering, Kyungnam University, Changwon 51767, Korea

Abstract To solve the problem of the uneven thickness distribution of a formed part caused by a large difference between the forming angles and the different curvatures of the surfaces in CNC incremental forming, a combinatorial optimization method of multidirectional sheet postures was proposed based on particle swarm optimization. In this method, an infinite number of optional sheet postures at each point in the forming area are taken as the combined object. The optimization goal is to make the forming angles of the entire sheet part be smaller than the forming limit angle and to minimize the difference between them; then find the optimal combination of the multidirectional sheet postures that can be selected at each point in the forming area. Case studies of the algorithm and the actual forming experiment show that not only can the optimized multidirectional sheet metal postures determined by the proposed method realize the non-fracture forming of the sheet metal parts with different forming angles and different curvature of the surface, but also obtain a more uniform thickness distribution of the formed parts.

1. Introduction

With the continuous advancement of computer science and technology, digital sheet metal forming technologies have begun to appear and continue to be developed. As a leader among them, the sheet metal CNC incremental forming technology has begun to develop rapidly in many fields and has been practically applied. Compared with traditional sheet metal forming technology, the reason that the sheet metal CNC incremental forming technology can obtain great advantages in the small batch production [1, 2] is mainly that the forming process does not need specific molds, its production cycle is greatly shortened, and the manufacturing cost is also greatly reduced [3, 4].

However, the sheet metal CNC incremental forming technology also inevitably has some disadvantages, such as uneven thickness distribution of the formed part and excessive thinning, which restricts its further popularization and application [5, 6].

To solve the problem, Zhang et al. [7] proposed a new hybrid flexible forming process. The forming process first makes a preform using the multi-point forming process, and then the preform is formed again using the single point incremental forming process again, which can improve the thickness distribution of the formed part to a certain extent. Parnika et al. [8] conducted a single point incremental forming experiment using preheating the sheet at different temperatures. The experimental result shows that the preheating can improve the wall thickness distribution to a certain extent and make the thickness more uniform. Choi and Lee [9] proposed a hybrid forming method combining the incremental forming and the stretch forming and established a mathematical model to predict the thickness distribution. The result shows that the hybrid forming method can improve the thickness distribution of the formed part. The above researches have improved the thickness distribution of the formed part to some extent, but the problems of uneven thickness distribution and excessive thinning of the difficult-forming

surfaces with large forming angles have not been solved because the traditional single incremental forming is still using horizontal sheet posture with the same layer spacing.

As we all know, in the process of the CNC incremental forming, the thickness of the sheet in the forming area depends on the forming angles, and the forming angles depend on the angle between the sheet and the surface of the sheet part [10, 11], so the problem of uneven thickness distribution and excessive thinning can be solved by changing the sheet posture or model posture.

Zhu et al. [12] proposed a method to control the forming angles and the thickness of the formed part by adjusting the target part posture (forming direction). However, in practice, the method has problems such as difficulty in clamping the sheet, difficult to fill the surface vacancies, and the need for special support. Moreover, for the multi-featured sheet metal, it is difficult to find a way to keep the sheet posture that can reduce the forming angles and minimize the difference relatively to all characteristic surfaces. Vanhove et al. [13] and Tanaka et al. [14] homogenized the thickness of the formed part based on the sheet posture that is inclined in a certain direction by taking the simple shapes such as the elliptical cones with different slopes between the left and right sides but also the shape is symmetrical between front and back sides as shown in Fig. 1.

Zhu et al. [15] generated the forming toolpath inclined in a certain direction using the genetic algorithm and adjusted the horizontal sheet posture to the inclined sheet posture, which made the difference between the forming angles of the left and right side surfaces to be smaller and to reduce the forming angles of the left side surface, so that the problem of excessive thinning of the thickness of the formed part can be solved. Zhu and Li [16] proposed a method to make the forming angles smaller than the forming limit angle by rotating the sheet posture, as shown in Fig. 2. The method only guaranteed that the forming angles on the surfaces were smaller than the forming limit angle, while did not make the sheet posture and the forming angles to be in an optimal state to homogenize the thickness of the formed part.

The research results mentioned above show that [12-16], the thickness of the formed part can be controlled through adjusting the sheet posture. But these studies only used an unoptimized multidirectional sheet posture that is only applicable to extremely special simple models with a certain difference of the forming angles between the left and right sides and the symmetrical shapes between the front and back sides, while it is difficult to make the sheet maintaining a reasonable posture relatively to the multi-features sheet part with different surface curvatures.

In response to the above problems, we proposed a new CNC incremental forming method based on the feature recognition and the multidirectional adjustment of the sheet posture in our previous research [17]. The method adopts the multidirectional sheet posture for the sheet metal part that is composed of many forming features with different geometric shapes. That is, the sheet metal part with multi-features is decomposed into a plurality of forming feature units according to the size and distribution of the forming angles using the feature recognition algorithm. Then the sheet postures are adjusted in real time by the extrusion movement of the forming tool so that different directional sheet postures are given to each forming feature units to make the forming angles on the surface less than the forming limit angle. Therefore, each forming feature unit can be individually formed to achieve non-rupture forming of the sheet part with large forming angles such as the straight wall, as shown in Fig. 3.

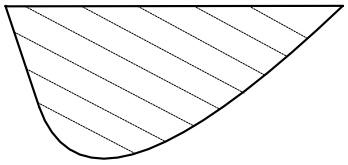

Fig. 1. Single orientation sheet posture.

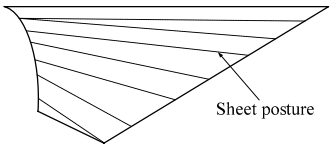

Fig. 2. Personalized sheet posture.

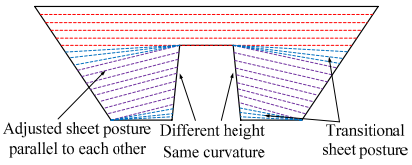

Fig. 3. Multidirectional sheet postures.

The key to the more effective function of this method is to reasonably determine the optimal combination of the multidirectional sheet postures that can minimize the thickness reduction and homogenize the thickness distribution of the formed part according to the infinite number of optional multidirectional sheet postures. However, this study [17] does not address the problem of the optimal combination of multidirectional and multiple sheet metal postures.

To this end, a combinatorial optimization method of the optimized multidirectional sheet posture for the formed part thickness homogenization based on the particle swarm optimization was proposed. The goal is to minimize the difference of the forming angles of the entire formed part and to obtain the optional combinatorial optimization of the multidirectional sheet postures to ensure that although the different orientations of the sheet postures are given to the forming area, but the difference of the forming angles can be minimized.

2. Combinatorial optimization method of the multidirectional sheet postures

The sheet metal CNC incremental forming based on the multidirectional adjustment of the sheet posture is to make the

sheet to be inclined from the surface with the large forming angles (difficult-forming surface) to the surface with the small forming angles (easy-forming surface) by the extrusion motion of the forming tool during the CNC incremental forming process, reducing the forming angles of the difficult-forming surface while increasing the forming angles of the easy-forming surface, and achieving non-rupture forming of the difficult-forming surface and homogenizing the thickness of the entire formed part.

For example, as shown in Fig. 4, the forming angles of the easy-forming surface and the difficult-forming surface are θ_1 and θ_3 before the sheet postures are adjusted; while after the sheet postures are adjusted, the forming angle of the easy-forming surface is increased from θ_1 to θ_2, and the forming angle of the difficult-forming surface is reduced from θ_3 to θ_4. At this time, the difference between θ_2 and θ_4 is significantly smaller than the difference between θ_1 and θ_3.

There are an infinite number optional sheet postures at each point of the forming area. In this paper, the optional sheet postures at each point in the forming area were taken as the combined object; the optimal combination of the sheet posture in the forming area was determined using particle swarm optimization by taking the minimization of the forming angle and the difference of the forming angles of the entire part surface as the optimization goal.

As shown in Fig. 5, the sheet posture on any layer is determined by the radial line on the corresponding contour ring according to the omnidirectional sheet posture generation algorithm proposed by Li [17], while the radial line is determined by controlling the ray from central point O_{ij} to point A_{ij} on the contour ring that intersects with the forming surface at point B_{ij}. For any radial line, the inclination angle is determined by θ_{ij}, so the sheet posture can be adjusted by controlling the size of θ_{ij} and the forming angles can be adjusted to be smaller than the forming limit angle $\theta_{\lim}$. The adjustment range of the adjustment angle θ_{ij} of the radial line is shown in Eq. (1).

$$\begin{cases} \theta_{ij} \geq \min(\theta_{\lim} - \alpha_{\text{initial}},\ \beta_{\text{initial}} - \theta_{\lim}) \\ \theta_{ij} \leq \max(\theta_{\lim} - \alpha_{\text{initial}},\ \beta_{\text{initial}} - \theta_{\lim}) \end{cases} \tag{1}$$

where α_{initial} represents the initial forming angle of the easily-forming surface, and β_{initial} represents the initial forming angle of the difficult-forming surface. Therefore, there are *n* kinds of radial lines to be chosen at any point on any layer, which can make the forming angles to be smaller than the forming limit angle within the range of the adjustment angle θ_{ij}. For all points on all layers, there are *n* kinds of choices at each point corresponding to *n* kinds of different sheet postures.

If it is not screened, any one of the optional schemes at each point is selected, it is inevitable that the thickness distribution is uneven although the sheet metal can be formed. In view of this situation, the paper proposed an optimal combination method of the optimized multidirectional sheet posture, which was taking into account the sheet postures at all points and using particle swarm optimization to optimize the radial line adjustment angle θ_{ij} at each point, then finding the optimal combination of sheet postures to minimize the thickness differences across the formed part.

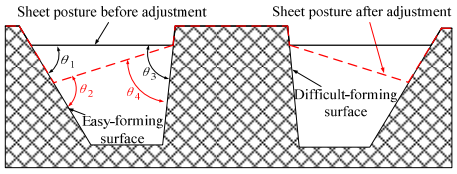

Fig. 4. Adjustment of the sheet posture.

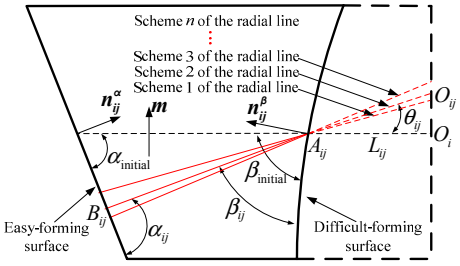

Fig. 5. Optional schemes of the radial line.

From the geometric relationship in Fig. 5, we can know the following formula.

$$\alpha_{ij} = \alpha_{ij}^{\text{initial}} + \theta_{ij} \tag{2}$$

$$\beta_{ij} = \beta_{ij}^{\text{initial}} - \theta_{ij} \tag{3}$$

where α_{ij} is the forming angle on the easy-forming surface of the sheet posture determined by the radial line at the *j*-th point on the *i*-th contour ring, and β_{ij} is the forming angle on the difficult-forming surface of the sheet posture determined by the radial line at the *j*-th point on the *i*-th contour ring; $\alpha_{ij}^{\text{initial}}$ is the initial forming angle on the easy-forming surface at the horizontal sheet posture, and $\beta_{ij}^{\text{initial}}$ is the initial forming angle on the difficult-forming surface at the horizontal sheet posture. For a formed part, $\beta_{ij}^{\text{initial}} > \alpha_{ij}^{\text{initial}}$. $\alpha_{ij}^{\text{initial}}$ and $\beta_{ij}^{\text{initial}}$ can be solved by the following formula:

$$\alpha_{ij}^{\text{initial}} = \cos^{-1} \frac{\boldsymbol{n}_{ij}^{\alpha} \cdot \boldsymbol{m}}{\left|\boldsymbol{n}_{ij}^{\alpha}\right| \cdot \left|\boldsymbol{m}\right|} \tag{4}$$

$$\beta_{ij}^{\text{initial}} = \cos^{-1} \frac{\boldsymbol{n}_{ij}^{\beta} \cdot \boldsymbol{m}}{\left|\boldsymbol{n}_{ij}^{\beta}\right| \cdot \left|\boldsymbol{m}\right|} \tag{5}$$

where, $\boldsymbol{n}_{ij}^{\alpha}$ is the normal vector of the triangular surface on the easy-forming surface where the point with the same height as the *j*-th point on the *i*-th contour line, and $\boldsymbol{n}_{ij}^{\beta}$ is the normal vector of the triangular surface on the difficult-forming surface where the point with the same height as the *j*-th point on the *i*-th contour line. $\boldsymbol{m}$ is the normal vector of the horizontal plane.

The difference between the two forming angles α_{ij} and β_{ij} determined by any sheet posture can be obtained by Eq. (6).

$$\gamma = \alpha_{ij} - \beta_{ij} = (\alpha_{ij}^{\text{initial}} + \theta_{ij}) - (\beta_{ij}^{\text{initial}} - \theta_{ij}) = \alpha_{ij}^{\text{initial}} - \beta_{ij}^{\text{initial}} + 2\theta_{ij} . \quad (6)$$

In this paper, the particle swarm optimization algorithm was used to determine the optimal combination of θ_{ij} to minimize γ value.

3. Solution of the sheet posture combination based on particle swarm optimization

The degree of the thickness uneven of the formed part is mainly determined by the difference between the forming angles of the forming surface. For any radial line, the difference between the forming angles α_{ij} and β_{ij} can be controlled by controlling the adjustment angle θ_{ij} of the radial line. Therefore, we aimed to find a set of forming angles with the minimum difference and the radial line adjustment angle θ_{ij} that minimizes the forming angles difference through the particle swarm optimization and then obtains a set of optimally combined sheet postures.

3.1 Basic principles of the particle swarm optimization

Particle swarm optimization (PSO) [18] is an effective optimization tool for the nonlinear continuous optimization problems, combinatorial optimization problems, and mixed integer nonlinear optimization problems [19]. The algorithm randomly generates an initial population at the initial stage and gives each particle an initial random velocity, and then continuously approaches the optimal solution based on the flight experience. The specific update method of the speed and position of each particle is shown as follows [20]:

$$v_i^d(t+1) = \omega v_i^d(t) + c_1 r_1[p_i^d(t) - x_i^d(t)] + c_2 r_2[p_g^d(t) - x_i^d(t)] \quad (7)$$

$$x_i^d(t+1) = x_i^d(t) + v_i^d(t+1) \quad (8)$$

$$\begin{cases} v_i^d = v_{\max}, & v_i^d > v_{\max} \\ v_i^d = -v_{\max}, & v_i^d < -v_{\max} \end{cases} \quad (9)$$

where i represents the particle in the population, $i = 1, 2, \cdots, N$, N represents the size of the population; d represents the space dimension, $d = 1, 2, \cdots, D$; t represents the iteration times of the algorithm, $t = 1, 2, \cdots, T_{max}$, T_{max} is the specified maximum times of iteration; c_1 and c_2 represent the acceleration constants of the particles; r_1 and r_2 are two random numbers uniformly distributed between [0,1]; x represents the spatial coordinate position; v represents the speed, and $v_{\max}$ is the specified maximum speed; the value of inertia weight ω is usually constant, and can also be adjusted dynamically. The specific expression is shown as follows:

$$\omega = \omega_{\max} - \frac{(\omega_{\max} - \omega_{\min}) \times t}{T_{\max}} . \quad (10)$$

3.2 Construction of the objective function

The optimization goal is to make the thickness of the formed part to be homogenized. Because the sheet thickness in the forming area depends on the forming angles, the optimization goal indirectly becomes to make the global forming angles to be smaller than the forming limit angle and to minimize the difference of the forming angles. The degree of the forming angles difference can be expressed by the variance.

The specific calculation formula of variance is shown as follows:

$$\sigma^2 = \frac{\sum (X - \mu)^2}{N} \quad (11)$$

where σ^2 is the population variance, X is the variable, μ is the population mean, and N is the population number. However, the sample statistics are used instead of the population parameters when the population mean is difficult to obtain in actual work. The sample variance calculation formula is shown as follows after correction:

$$S^2 = \frac{1}{n-1} \sum_{i=1}^{n} (x_i - \overline{X})^2 \quad (12)$$

$$\overline{X} = \frac{x_1 + x_2 + \cdots + x_n}{n} \quad (13)$$

where S^2 is the sample variance, $x_i(x_1, x_2, \cdots, x_n)$ is the variable, $\overline{X}$ is the sample mean, and n is the number of samples. The global objective function is constructed by taking the α_{ij} and β_{ij} as the independent variables.

$$f(x) = \frac{1}{n-1} \sum_{i=1}^{n} (x_i - \overline{X})^2 \quad (14)$$

where x_i includes all α_{ij} and β_{ij} determined by the radial line, and $\overline{X}$ is the sample mean of all α_{ij} and β_{ij}. Eq. (14) can be transformed as follows.

$$f(x) = \frac{1}{2n-1} \sum_{i=1}^{n} [(x_i^1 - \overline{X})^2 + (x_i^2 - \overline{X})^2] \quad (15)$$

where x_i^1 represents α_{ij}, x_i^2 represents β_{ij}. The expression of $\overline{X}$ is as follows:

$$\overline{X} = \frac{\sum_{i=1}^{n} (x_i^1 + x_i^2)}{2n} . \quad (16)$$

Putting Eqs. (2) and (3) into Eq. (16), the expression of $\overline{X}$ is as follows:

$$\overline{X} = \frac{\sum \alpha_{ij}^{\text{initial}} + \sum \beta_{ij}^{\text{initial}}}{2n} . \quad (17)$$

Since the $\alpha_{ij}^{\text{initial}}$ and $\beta_{ij}^{\text{initial}}$ have already been determined for the given the model, the $\overline{X}$ is a fixed value, making $C = \overline{X}$, then Eq. (15) can be transformed as follows:

$$f(x) = \frac{1}{2n-1}\sum_{i=1}^{n}[(x_i^1 - C)^2 + (x_i^2 - C)^2]. \tag{18}$$

The initial random value of the adjustment angle θ_{ij} is given by the PSO, and the α_{ij} and β_{ij} corresponding to θ_{ij} are obtained from the Eqs. (2) and (3), and then taken to find the degree of difference of the forming angles using the Eq. (18).

3.3 Construction of the fitness function

The fitness function refers to the ability of the individual to adapt to the environment and survive. The greater the fitness value, the stronger the survivability. Otherwise, the lower the fitness value, the weaker the survivability. The fitness function is usually transformed from the objective function and the fitness value must be non-negative. The goal of the optimal combination of the sheet posture is to minimize the difference of the forming angles, which is a problem of minimizing the objective function, so the following fitness function $Fit(X)$ is used:

$$Fit(X) = \frac{1}{1 + c + f(x)} \quad c \geq 0, c + f(x) \geq 0 \tag{19}$$

where c is a constant. Take $c = 0$ to ensure $c + f(x) \geq 0$. Putting $f(x)$ into Eq. (19).

$$Fit(X) = \frac{1}{1 + \frac{1}{2n-1}\sum_{i=1}^{n}[(x_i^1 - C)^2 + (x_i^2 - C)^2]}. \tag{20}$$

3.4 Constraint condition

First, all the forming angles must be smaller than the preset forming limit angle.

$$x_i \leq \theta_{\lim}. \tag{21}$$

Secondly, it actually controls the forming angles α_{ij} and β_{ij} by controlling the adjustment angle θ_{ij} of the radial line although the objective function $f(x)$ takes the forming angles α_{ij} and β_{ij} as independent variables, so the size of θ_{ij} needs to be controlled. Since all forming angles need to be smaller than the forming limit angle after adjustment, it can be obtained from Eqs. (2), (3) and (21) as follows:

$$\alpha_{ij}^{\text{initial}} + \theta_{ij} < \theta_{\lim} \tag{22}$$

$$\beta_{ij}^{\text{initial}} - \theta_{ij} < \theta_{\lim}. \tag{23}$$

Table 1. Reference value of the acceleration constant.

Scholar	c_1 and c_2
Clerc	$c_1 = c_2 = 2.05$
Carlisle	$c_1 = 2.8$, $c_2 = 1.3$
Trelea	$\omega = 0.6$, $c_1 = c_2 = 1.7$
Eberhart	$\omega = 0.729$, $c_1 = c_2 = 1.494$

From Eqs. (22) and (23), the range of θ_{ij} can be obtained as follows.

$$\beta_{ij}^{\text{initial}} - \theta_{\lim} < \theta_{ij} < \theta_{\lim} - \alpha_{ij}^{\text{initial}}. \tag{24}$$

That is, it needs to initialize θ_{ij} within the range.

3.5 Solution process

The process of solving the optimal combination of the sheet posture using PSO is as follows.

(1) The population initialized

The main parameters that need to be initialized in the population include the number of particles *N*, the inertia factor ω, the maximum flying speed $v_{\max}$, the acceleration constants c_1 and c_2, and the maximum times of iterations. The number of the particles *N* is generally 20 to 40, then 100 to 200 particles are also needed for the special problems. The larger the number of particles, the easier it is to find the global optimal solution, but at the same time the search time is longer. We took *N* = 40, that is, the group consists of 40 individuals. The inertia factor ω can be a variable or a constant. If ω is a variable, it is usually set to a large value at the beginning and then gradually decreased during the iteration process, in which Eq. (10) can be used; if it is constant, a reasonable value in the range of 0.6 to 0.75 is recommended. We took $\omega = 0.6$. Acceleration constants c_1 and c_2 usually take values between [0, 2]. At present, there are bifurcations of values for the two parameters in academic circles.

Table 1 shows the reference values given by the major scholars [21]. Among them, the first and fourth applications are more common. We took $c_1 = c_2 = 2.0$.

If the maximum speed $v_{\max}$ is a fixed value, it is usually set from 10 % to 20 % of the variation range per dimension. We took $v_{\max} = 0.8$. The maximum times of iterations usually take from 100 to 4000 which is determined according to the needs. The maximum times of iterations in this paper is 100.

(2) Calculate the fitness value of each particle

Calculate the initial fitness value of each particle according to the initial particle position, take it as the local optimal value *pbest* of each particle and remember the location; take the best initial fitness value as the current global optimal value *gbest* and remember the location.

(3) Update the flight speed

Update the current flying speed of each particle according to Eq. (7).

(4) The flying speed limitation

Limit the maximum flying speed of each particle according to Eq. (9).

(5) Update the particle position

Update the current location of each particle according to Eq. (8).

(6) Update the local optimal value *pbest*

Calculate the current fitness value of each particle again and compare it with the historical local optimal value. If the current fitness value is better than the historical local optimal value, take the current fitness value as the particle's local optimal value *pbest*, and take the corresponding position as the local optimal location.

(7) Update the global optimal value *gbest*

The global optimal value found in the current population is the new global optimal value *gbest* and the corresponding position is taken as the global optimal value location.

(8) Iterative

Repeat steps (3)~(7) until the iteration termination condition is satisfied.

(9) Output

Output the global optimal value of the particles in the population and the corresponding particle positions, that is, the radial line adjustment angle θ_{ij} and the forming angles α_{ij} and β_{ij} after adjustment.

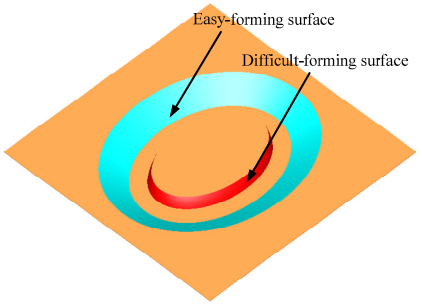

Fig. 6. Model used for verification.

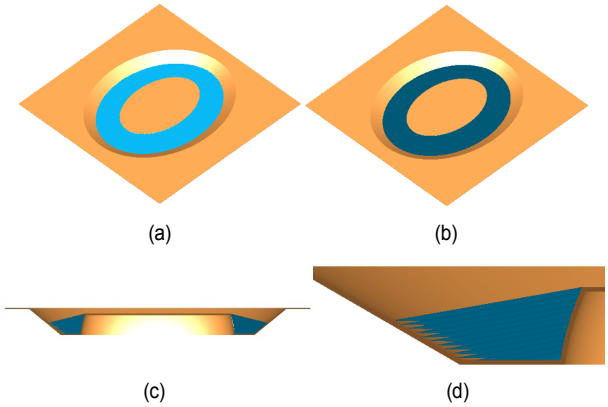

Fig. 7. Unoptimized multidirectional sheet posture: (a) multidirectional radial line; (b) multidirectional sheet posture; (c) section view; (d) local enlarged view.

4. Case studies

To verify the feasibility of the algorithm proposed in this paper, a sheet posture optimization software system based on PSO was developed using C++, VC++, OpenGL and MATLAB under the Windows 7 environment, and the case studies were given as follows by taking the sheet metal model shown in Fig. 6 as example.

The curvature of the difficult-forming surface of the model gradually changes in the Z-axis direction, and the forming angles are different from each other. When the sheet is in a horizontal posture, the forming angle of the easy-forming surface is 30.0025°; the difficult-forming surface is divided into 12 layers from top to bottom according to the layer spacing of 1.1 mm, and the forming angles from the first layer to the twelfth layer are 67.1620°, 68.2545°, 69.1813°, 71.0447°, 71.9813°, 72.9056°, 73.8420°, 75.7958°, 76.7758°, 77.7536°, 78.5322° and 80.1836°, respectively. The minimum forming angle is 30.0025° and the maximum forming angle is 80.1836° of the model. The forming angles on the difficult-forming surface are greater than the forming limit angle of 65°, and the difference between the maximum forming angle and the minimum forming angle is 50.1811°.

When using unoptimized multidirectional sheet posture for forming, the forming angle on the easy-forming surface is 40.0025°; the forming angles on the difficult-forming surface are 57.1620°, 58.2545°, 59.1813°, 61.0447°, 61.9813°, 62.9056°, 63.8420°, 65.7958°, 66.7758°, 67.7536°, 68.5322° and 70.1836°, respectively. The minimum forming angle is 40.0025° and the maximum forming angle is 70.1836° at this time. There are still forming angles greater than the forming limit angle on the difficult-forming surface, and the difference between the maximum forming angle and the minimum forming angle is 30.1811°. Fig. 7 shows the unoptimized multidirectional radial line and the sheet posture.

The objective function value reached a minimum value of 38.1258 after 40 iterations and stabilized by the PSO. The image where the particle's flying position changed with the times of iterations is shown in Fig. 8, and the image where the objective function value changed with the times of iterations is shown in Fig. 9.

When the value of the objective function reached the minimum value, the sixth set of data in the 40 groups of samples shown in Fig. 10 is the optimal adjustment angle of the radial lines of each layer, which are 18.6463°, 19.1251°, 19.5527°, 20.5194°, 20.9748°, 21.4304°, 21.9403°, 22.8861°, 23.3443°, 23.8963°, 24.2505° and 25.1203° from top to bottom.

The forming angles of the easy-forming surface shown in Fig. 11 after adjusting according to the optimal adjustment angle of the radial line become 48.6463°, 49.1251°, 49.5527°, 50.5194°, 50.9748°, 51.4304°, 51.9403°, 52.8861°, 53.3443°, 53.8963°,

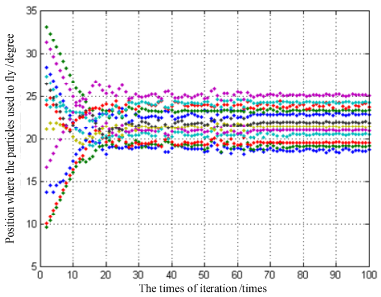

Fig. 8. Image of particle's flying position changing with the times of iteration.

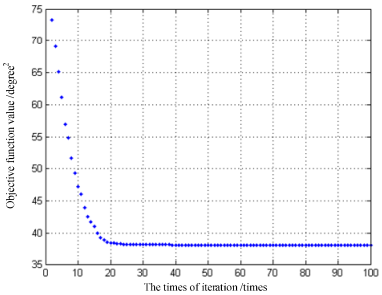

Fig. 9. Image of objective function value changing with the times of iteration.

54.2505° and 55.1203°, respectively.

The forming angles of the difficult-forming surface shown in Fig. 12 after adjusting according to the optimal adjustment angle of the radial line become 48.5157°, 49.1294°, 49.6286°, 50.5253°, 51.0065°, 51.4752°, 51.9017°, 52.9097°, 53.4315°, 53.8573°, 54.2817° and 55.0633°, respectively.

The minimum forming angle and maximum forming angle are 48.5157° and 55.1203° after the multidirectional sheet postures have been optimized, which are both smaller than the forming limit angle 65°, and the difference between the maximum forming angle and the minimum forming angle is 6.6046°. Compared with the unoptimized multidirectional sheet posture, not only the forming angles on the difficult-forming surface are adjusted to be smaller than the forming limit angle, but the difference between the maximum forming angle and the minimum forming angle is greatly reduced from 30.1811° when not optimized to 6.6046° after optimized. Therefore, the algorithm proposed in this paper effectively optimizes the forming angle of the sheet metal during the incremental forming process and reduces the difference between the forming angles. Fig. 13 shows the multidirectional radial line and the sheet posture generated according to the optimal radial line adjustment angle; Fig. 13(a) shows the multidirectional radial line generated according to the optimized radial line adjustment angle; Fig. 13(b) shows the optimized multidirectional sheet posture generated according to the radial line. Figs. 13(c) and (d) show the cutaway view of the optimized multidirectional sheet posture and the partial enlarged drawing of the sheet posture, respectively.

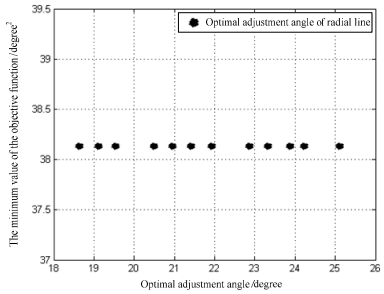

Fig. 10. Optimal adjustment angle of the radial line.

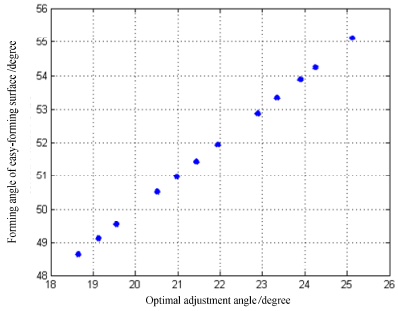

Fig. 11. Forming angles on the easy-forming surface after adjustment.

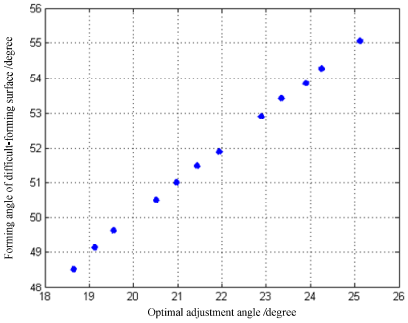

Fig. 12. Forming angles on the difficult-forming surface after adjustment.

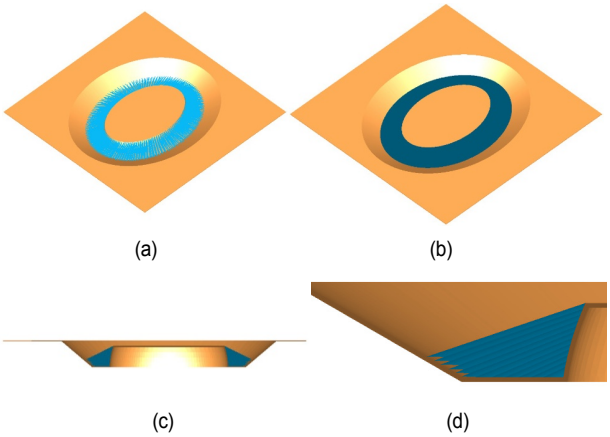

Fig. 13. Optimized multidirectional sheet posture: (a) multidirectional radial line; (b) multidirectional sheet posture; (c) section view; (d) local enlarged view.

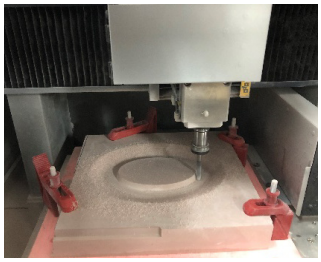

Fig. 14. The milling process of the support.

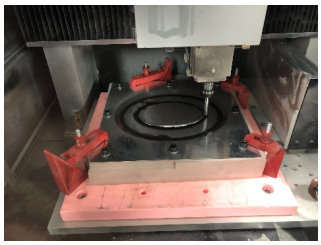

(a)

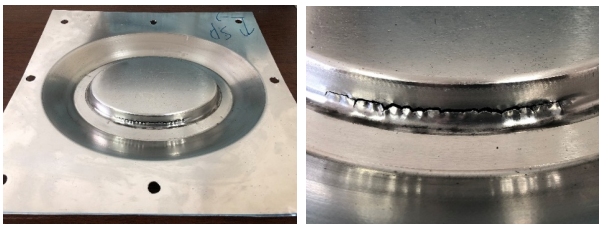

(b) (c)

Fig. 15. Horizontal sheet posture: (a) forming process; (b) formed part; (c) local enlarged view.

5. Forming experiment

To verify the feasibility of the proposed method, taking the model shown in Fig. 6 as research object, the forming experiments were carried out by using the forming method based on the horizontal multidirectional sheet posture, unoptimized multidirectional sheet posture, and optimized multidirectional sheet posture. The the support was milled by a mold engraving machine as shown in Fig. 14. In the forming experiment, the sheet material was 1060 aluminum plate and the thickness was 0.88 mm. The forming tool was a hemispherical tool head with a diameter of 10 mm. The spindle speed and the feed rate was set as 400 r/min and 600 mm/min.

Fig. 15(a) shows the CNC incremental forming process based on the horizontal sheet posture. When the forming process was conducted to a depth of 15 mm, cracks and rupture began to appear on the difficult-forming surface as shown in Figs. 15(b) and (c). The forming experiment showed that the sheet part cannot be formed using the horizontal sheet posture. Figs. 16(a) and (b) showed the CNC incremental forming process and the formed part by using the optimized multidirectional sheet posture. The formed part was partially broken at a depth of 16 mm as shown in Fig. 16(c). The CNC incremental forming process and the formed part based on the optimized multi-

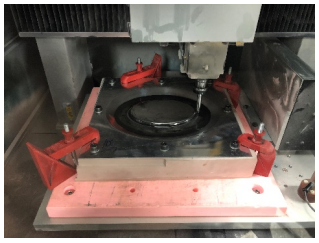

(a)

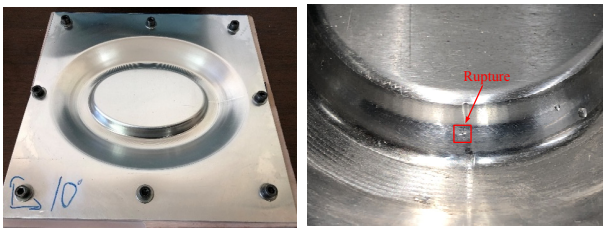

(b) (c)

Fig. 16. Unoptimized multidirectional sheet posture: (a) forming process; (b) formed part; (c) local enlarged view.

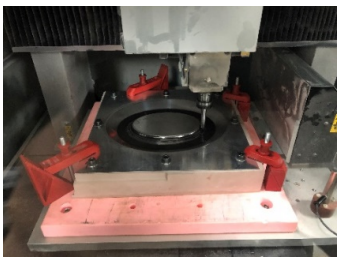

(a)

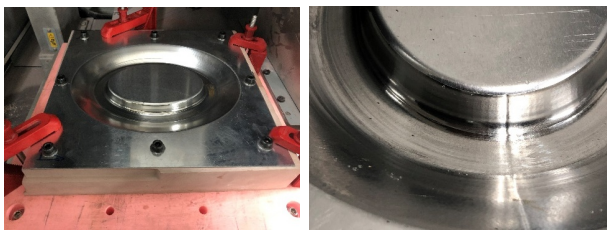

(b) (c)

Fig. 17. Optimized multidirectional sheet posture: (a) forming process; (b) formed part; (c) local enlarged view.

directional sheet posture are shown in Figs. 17(a) and (b). The formed part had good forming quality without cracking as shown in Fig. 17(c).

To compare the profile accuracy of the formed parts with the unoptimized multidirectional sheet posture and optimized multidirectional sheet posture, the profile measurement at $Y = 0$ section of the formed part was carried out by using the three-coordinate measuring machine at an interval of 2 mm as shown in Fig. 18. Import the profile data obtained from the measurement into the Excel software and draw the profile curves which are shown in Fig. 19. Then compare it with the profile curve of the theoretical model at $Y = 0$ section and draw the Z-direction deviation curves as shown in Fig. 20.

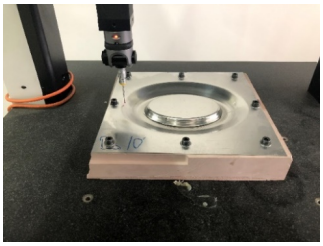

Fig. 18. The profile measurement of the formed part.

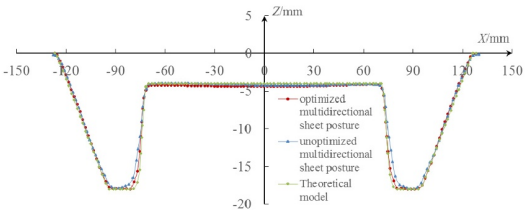

Fig. 19. The profile curve at $Y = 0$ section.

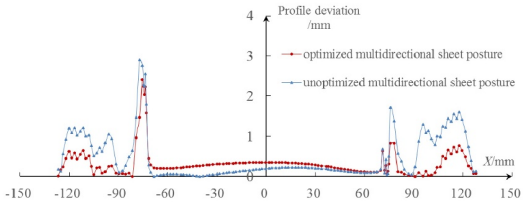

Fig. 20. Z-direction deviation.

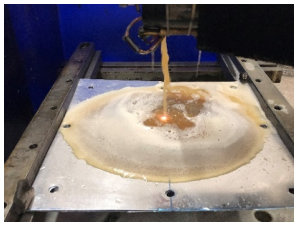

(a)

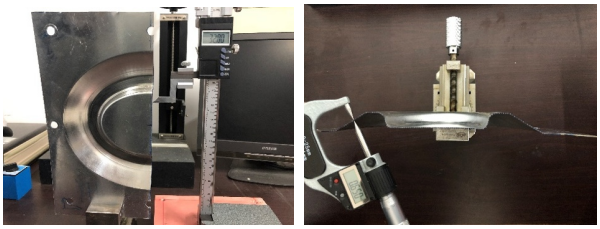

(b) (c)

Fig. 21. Thickness measurement of the formed part: (a) cutting process; (b) marking sample points; (c) thickness measurement of sample points.

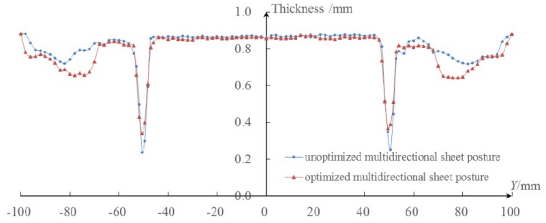

Fig. 22. Comparison of the thickness distribution of the formed parts at $X = 0$ section.

It can be known from Figs. 19 and 20 that the maximum Z-direction deviation of the formed part obtained by using the unoptimized multidirectional sheet posture is 2.9032 mm, the minimum Z-direction deviation is 0.0011 mm, and the average deviation is 0.5189 mm. The maximum Z-direction deviation of the formed part obtained by using the optimized multidirectional sheet posture is 2.4201 mm, the minimum Z-direction deviation is 0.0001 mm, and the average deviation is 0.3563 mm. It can be known that the profile of the formed part obtained by the optimized multidirectional sheet posture is more consistent with the theoretical profile.

To compare and analyze the thickness of the formed parts obtained by using the unoptimized multidirectional sheet posture and optimized multidirectional sheet posture, a wire cutting machine was used to cut the formed parts along the $X = 0$ section and to measure the thickness of the corresponding sections, as shown in Fig. 21(a). One half of the formed parts are selected after cutting and marked along the cross section from the bottom to top with a height meter at intervals of 2 mm as shown in Fig. 21(b). Then the pointed micrometer is used to measure the thickness of the marking points as shown in Fig. 21(c).

The measured data was imported into the Excel software and the thickness distribution curves were plotted. The comparison of the thickness distribution of the formed parts based on the unoptimized multidirectional sheet posture and optimized multidirectional sheet posture is shown in Fig. 22. The thickness of the formed part based on the horizontal sheet posture is mainly distributed in the range of 0.252 mm to 0.863 mm, and the overall thickness difference is 0.611 mm. The thickness of the easy-forming surface is mainly distributed in the range of 0.780 mm to 0.721 mm, while the thickness of the difficult-forming surface is mainly distributed in the range of 0.237 mm to 0.746 mm, and the thickness difference between the difficult-forming surface and easy-forming surface is 0.543 mm. The thickness of the formed part obtained by the optimized multidirectional sheet posture is mainly distributed in the range of 0.338 mm to 0.829 mm, and the overall thickness difference is 0.491 mm. The thickness of the easy-forming surface is mainly distributed in the range of 0.641 mm to 0.722 mm, while the thickness of the difficult-forming surface is mainly distributed in the range of 0.338 mm to 0.657 mm, and the thickness difference between the difficult-forming surface and easy-forming surface is 0.384 mm. From the above data, the thickness of the formed part is more uniform when the sheet is formed by using the optimized multidirectional sheet posture.

The roughness measurement was performed as shown in Fig. 23(a). Figs. 23(b) and (c) show the roughness curves of

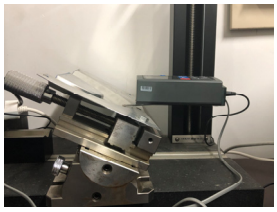

(a)

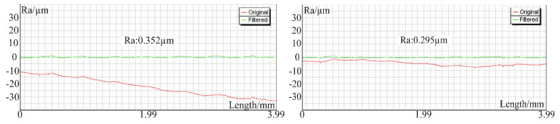

(b) (c)

Fig. 23. The roughness measurement: (a) measurement process; (b) unoptimized multidirectional sheet posture; (c) optimized multidirectional sheet posture.

formed parts based on the optimized and unoptimized multidirectional sheet posture, respectively, which show that the surface roughness of the formed part obtained by the optimized multidirectional sheet posture is better.

6. Conclusion

To make CNC incremental forming based on the multidirectional adjustment of the sheet posture work better, a combinatorial optimization method of the optimized multidirectional sheet posture for the formed part thickness uniformity based on PSO was proposed in this paper. The research result shows not only that the proposed method can achieve non-crack forming of the sheet metal part with large difference forming angles and different curvatures of the surface, but also obtain a more uniform thickness distribution of the formed part. The CNC incremental forming method based on the combinatorial optimization of the optimized multidirectional sheet posture proposed in the paper can effectively solve the problem of the thickness distribution unevenness of the formed part due to the large difference between the forming angles, which is significant to the development of CNC incremental forming technology. In the future study, for the combinatorial optimization of the optimized multidirectional sheet posture, it is necessary to continue to study the influence on the forming quality of the extrusion direction of the forming tool.

Conflict of interest

The authors declare that they have no conflict of interest.

Nomenclature

O_{ij} : The central point of the radial line
θ_{ij} : The angle of inclination of the radial line
$\theta_{\lim}$: Forming limit angle
α_{initial} : The initial forming angle of the easily-forming surface
β_{initial} : The initial forming angle of the difficult-forming surface
α_{ij} : The forming angle on the easy-forming surface
β_{ij} : The forming angle on the difficult-forming surface
$\boldsymbol{m}$: The normal vector of the horizontal plane
i : The particle in the population
d : The space dimension
t : The iteration times of the algorithm
c_1, c_2 : The acceleration constants of the particles
r_1, r_2 : The random numbers uniformly distributed between [0,1]

References

[1] H. Wang, Y. B. Gu, X. Z. Guo, H. T. Wang, J. Tao and Y. Xu, Microstructure and mechanical properties of 2060-T8 Al-Li alloy after warm incremental forming, *Journal of Mechanical Science and Technology*, 32 (10) (2018) 4801-4812.

[2] S. Torsakul and N. Kuptasthien, Effects of three parameters on forming force of the single point incremental forming process, *Journal of Mechanical Science and Technology*, 33 (6) (2019) 2817-2823.

[3] Y. L. Li, X. X. Chen, Z. B. Liu, J. Sun, F. Li, J. F. Li and G. Q. Zhao, A review on the recent development of incremental sheet-forming process, *Int. J. Adv. Manuf. Technol.*, 92 (5-8) (2017) 2439-2462.

[4] J. R. Duflou, A. M. Habraken, J. Cao, R. Malhotra, M. Bambach, D. Adams, H. Vanhove, A. Mohammadi and J. Jeswiet, Single point incremental forming: state-of-the-art and prospects, *Int. J. Mater Form*, 11 (6) (2018) 743-773.

[5] A. K. Behera, R. A. de Sousa, G. Ingarao and V. Oleksik, Single point incremental forming: An assessment of the progress and technology trends from 2005 to 2015, *J. of Manuf Process*, 27 (2017) 37-62.

[6] G. Ambrogio, L. Filice, M. Gaudioso and G. L. Manco, Optimized tool-path design to reduce thinning in ISF process, *Int. J. Mater Form*, 3 (1) (2010) 959-962.

[7] H. Zhang, B. Lu, J. Chen, S. L. Feng, Z. Q. Li and H. Long, Thickness control in a new flexible hybrid incremental sheet forming process, *Proc. Inst. Mech. Eng., Part B*, 231 (5) (2017) 779-791.

[8] S. Parnika, K. Pavan, T. Puneet and P. Alexander, Improvement in formability and geometrical accuracy of incrementally formed AA1050 sheets by microstructure and texture reformation through preheating, and their FEA and experimental validation, *J. Braz Soc. of Mech. Sci. Eng.*, 40 (7) (2018) 335-349.

[9] H. Choi and C. Lee, A mathematical model to predict thickness distribution and formability of incremental forming combined with stretch forming, *Rob Comput-Integr Manuf.*, 55 (Part B) (2019) 164-172.

[10] D. Maheshwar and K. Vinayak, The effect of process parameters on forming forces in single point incremental forming, *Procedia Manuf.*, 29 (2019) 120-128.

[11] M. Sathish and K. C. Udaiyakumar, Experimental investigation and analytical model for improving the thickness distribution in multi-point incremental forming in sheet metal, *Mater Today: Proc.*, 5 (2) (2018) 12045-12055.

[12] H. Zhu, J. Ju and J. L. Bai, Research on the forming direction

optimization for the uniformity of the sheet part thickness in the CNC incremental forming, *Int. J. Adv. Manuf. Technol.*, 93 (5-8) (2017) 2547-2559.
[13] H. Vanhove, J. Gu, H. Sol and J. R. Duflou, Process window extension for incremental forming through optimal work plane rotation, *Spec Ed: 10th Int Conf Technol Plast* (2011) 508-512.
[14] S. Tanaka, K. Hayakawa and T. Nakamura, Incremental sheet forming with direction control of path planes, *Spec Ed: 10th Int Conf Technol Plast* (2011) 503-507.
[15] H. Zhu, J. Ju and J. L. Bai, Sheet thickness homogenization in CNC incremental forming based on tilted forming path, *Comput. Integr. Manuf. Syst.*, 24 (3) (2018) 631-638.
[16] H. Zhu and H. Y. Li, 5-Axis CNC incremental forming toolpath generation based on formability, *Int. J. Adv. Manuf. Technol.*, 94 (1-4) (2018) 1061-1072.
[17] J. L. Li, *Research on CNC Incremental Forming based on Multi-direction Real-time Adjustment of Sheet Posture*, Shenyang: Shenyang Aerospace University (2019).
[18] Y. M. Liu and B. Niu, *The Theory and Practice of New Particle Swarm Optimization*, Beijing: Science Press (2013).
[19] Z. Ji, H. L. Liao and Q. H. Wu, *Particle Swarm Optimization and Its Application*, Beijing: Science Press (2010).
[20] Q. K. Zhang, *Research on the Particle Swarm Optimization and Differential Evolution Algorithms*, Shandong: Shandong University (2017).
[21] J. W. Zhuo, Y. S. Wei, J. Qin and B. W. Li, *Application of MATLAB in Mathematical Modeling*, Beijing: Beihang University Press (2011).

Hu Zhu is a Professor in the College of Mechanical and Electrical Engineering at Shenyang Aerospace University. He received his B.S. from Jilin University, and M.S. and Ph.D. in the Department of Mechanical Design and Production Engineering at Seoul National University. His current research interests include CAD/CAM, 3D printing, CNC incremental forming.

Yang Wang is currently an M.S. student in the College of Mechanical and Electrical Engineering at Shenyang Aerospace University. He received his B.S. from the Mechanical Manufacturing and Automation at Shenyang Aerospace University. His research interests include CAD/CAM, CNC incremental forming.

Jaeguan Kang is currently a Professor of Mechanical Engineering at the Kyungnam University. He received his Ph.D. from Pohang University of Science and Technology, M.S. from Korea Advanced Institute of Science and Technology, B.S. from Seoul National University. His primary research interests include CAD/CAM, Incremental sheet metal forming.